View metadata, citation and similar papers at core.ac.uk

brought to you by CORE

provided by Elsevier - Publisher Connector

Biochimica et Biophysica Acta 1853 (2015) 233–243

Contents lists available at ScienceDirect

Biochimica et Biophysica Acta

journal homepage: www.elsevier.com/locate/bbamcr

STIM1 phosphorylation triggered by epidermal growth factor mediates cell migration

Vanessa Casas-Rua [a], Patricia Tomas-Martin [a], Aida M. Lopez-Guerrero [a], Ignacio S. Alvarez [b], Eulalia Pozo-Guisado [a,*], Francisco Javier Martin-Romero [a,*]

[a] Department of Biochemistry and Molecular Biology, School of Life Sciences, University of Extremadura, Badajoz, Spain
[b] Department of Cell Biology, School of Life Sciences, University of Extremadura, Badajoz, Spain

ARTICLE INFO

Article history:
Received 2 August 2014
Received in revised form 27 October 2014
Accepted 29 October 2014
Available online 4 November 2014

Keywords:
Calcium
EGF
ERK1/2
Migration
Phosphorylation
STIM1

ABSTRACT

STIM1 is a key regulator of store-operated calcium entry (SOCE), and therefore a mediator of Ca^{2+} entry-dependent cellular events. Phosphorylation of STIM1 at ERK1/2 target sites has been described as enhancing STIM1 activation during intracellular Ca^{2+} emptying triggered by the inhibition of the sarco(endo)plasmic Ca^{2+}-ATPase with thapsigargin. However, no physiological function is known for this specific phosphorylation. The present study examined the role of STIM1 phosphorylation in cell signaling triggered by EGF. Using a human endometrial adenocarcinoma cell line (Ishikawa cells) EGF or H-Ras(G12V), an active mutant of H-Ras, was found to trigger STIM1 phosphorylation at residues Ser575, Ser608, and Ser621, and this process was sensitive to PD0325901, an inhibitor of ERK1/2. Both, ERK1/2 activation and STIM1 phosphorylation took place in the absence of extracellular Ca^{2+}, indicating that both events are upstream steps for Ca^{2+} entry activation. Also, EGF triggered the dissociation of STIM1 from EB1 (a regulator of microtubule plus-ends) in a manner similar to that reported for the activation of STIM1 by thapsigargin. Migration of the Ishikawa cells was impaired when STIM1 phosphorylation was targeted by Ser-to-Ala substitution mutation of ERK1/2 target sites. This effect was also observed with the Ca^{2+} channel blocker SKF96365. Phosphomimetic mutation of STIM1 restored the migration to levels similar to that found for STIM1-wild type. Finally, the increased vimentin expression and relocalization of E-cadherin triggered by EGF were largely inhibited by targeting STIM1 phosphorylation, while STIM1-S575E/S608E/S621E normalized the profiles of these two EMT markers.

© 2014 Elsevier B.V. All rights reserved.

1. Introduction

Stromal interaction molecule (STIM1) is a single transmembrane endoplasmic reticulum protein that activates plasma membrane Ca^{2+} channels on the occurrence of conditions that trigger Ca^{2+} depletion in the endoplasmic reticulum [1]. Transient reduction in the intraluminal Ca^{2+} levels leads to Ca^{2+} dissociation from the EF-hand domain of STIM1, triggering its multimerization. STIM1 clustering precedes its relocalization underneath the plasma membrane where it activates Ca^{2+} entry through store-operated Ca^{2+} channels [2,3]. Ca^{2+} channels activated by STIM1 include some members of the TRPC channel family, and ORAI channels [4,5], including ORAI1 (also called CRACM1), a highly selective Ca^{2+} channel responsible for the Ca^{2+}-release-activated Ca^{2+} current (I_{CRAC}) [6]. STIM1 is therefore a key regulator of Ca^{2+} entry (SOCE), and its role in physiological and pathological events that are mediated by Ca^{2+} mobilization is currently under investigation. In this regard, it is known that STIM1 participates in the signaling that regulates cell migration [7], and recent evidence supports a role for Ca^{2+} entry in non-tumor cell proliferation [8–10], as well as in cell adhesion, migration, and proliferation in a number of tumor cell types [11–14]. Indeed, the increase of the cytosolic free Ca^{2+} concentration ($[Ca^{2+}]_i$) activates the Ca^{2+}-regulated protease calpain and the Ca^{2+}-stimulated protein tyrosine kinase 2 beta (PTK2B or PYK2) [12], a known regulator of focal adhesion dynamics. Consequently, the use of Ca^{2+} channel blockers or the knockdown of STIM1 or ORAI channels reduces proliferation and promotes cell cycle arrest in different tumor cell lines [11–17], indicating that SOCE may be a potential target in cancer therapy. The mechanisms of STIM1 activation thus need to be addressed in order to define potential new cancer treatment strategies.

One of the mechanisms that mediate the activation of STIM1 is the unfolding of the protein in response to store depletion into an open conformation that exposes a STIM1–ORAI1 activating region (SOAR) and allows it to interact with ORAI1 [18,19]. Another mechanism that

Abbreviations: EGF, epidermal growth factor; ER, endoplasmic reticulum; EMT, epithelial–mesenchymal transition; ERK, extracellular signal-regulated kinase; SOCE, store-operated Ca^{2+} entry

* Corresponding authors at: Department of Biochemistry and Molecular Biology, School of Life Sciences, University of Extremadura, Avenida de Elvas s/n. 06006-Badajoz, Spain. Fax: +34 924 289419.
E-mail addresses: epozo@unex.es (E. Pozo-Guisado), fjmartin@unex.es (F.J. Martin-Romero).

http://dx.doi.org/10.1016/j.bbamcr.2014.10.027
0167-4889/© 2014 Elsevier B.V. All rights reserved.

has been shown to be involved in the regulation of STIM1 is the phosphorylation of the protein. The full set of phosphoresidues has already been listed [20–22], and we have previously described how STIM1 activity is modulated by ERK1/2-dependent phosphorylation at residues Ser575, Ser608, and Ser621 [22]. Constitutive dephosphorylation of these residues impairs SOCE [22], whereas simulation of constitutive phosphorylation of STIM1 by means of Ser-to-Glu mutation of the aforementioned residues enhances STIM1 multimerization and SOCE in response to Ca^{2+} store depletion [23]. In our previous reports, STIM1 phosphorylation was observed under treatment with thapsigargin, a specific sarco(endo)plasmic reticulum Ca^{2+}-ATPase (SERCA) inhibitor [24], that triggered ERK1/2 activation. Conversely, restoration of intraluminal Ca^{2+} levels led to STIM1 dephosphorylation [23], suggesting a role for as yet undescribed phosphatases in the regulation of STIM1 inactivation.

In addition to ORAI1 and other proteins such as TRPC1 and SERCA (reviewed in [25]), STIM1 directly binds to the microtubule plus-end tracking protein EB1 (end-binding protein 1) [26], a protein that regulates microtubule-growing ends [27,28]. Later, we demonstrated that STIM1 phosphorylation at ERK1/2 sites leads to the dissociation of STIM1 from EB1 [23], and that this dissociation enables the multimerization of STIM1 in microtubule-independent and immobile clusters that activate Ca^{2+} channels and Ca^{2+} entry [23]. However, little is known regarding the phosphorylation of STIM1 upon physiological stimuli. ERK1/2 becomes activated by the Ras–Raf–MEK–ERK pathway in response to a number of stimuli, including the activation of the epidermal growth factor (EGF) receptor [29,30]. Thus, the treatment of cells with EGF provides an opportunity to study the role of STIM1 phosphorylation in response to the activation of this specific signaling pathway. Furthermore, EGF triggers a chemotactic response in tumor cells [31], and is involved in the *in vitro* epithelial–mesenchymal transition (EMT) in other cell types [32,33].

Because constitutive dephosphorylation of STIM1 at ERK1/2 target sites impairs SOCE [22], we hypothesized that phosphorylation of STIM1 could regulate cell migration. To test this hypothesis, we investigated the phosphorylation profile of STIM1 in cells upon stimulation with EGF. Using Ishikawa cells, which derive from an endometrial adenocarcinoma [34], in the present report we demonstrate that EGF triggers a significant phosphorylation of STIM1 at residues Ser575, Ser608, and Ser621. We also show here the critical role of STIM1 phosphorylation at ERK1/2 target sites in cell migration. Ser-to-Ala mutation of target residues or inhibition of STIM1 phosphorylation by ERK1/2 was found to impair both EGF-dependent chemotaxis and the epithelial–mesenchymal transition (EMT) triggered by EGF. On the contrary, constitutive phosphorylation significantly promoted migration and EMT, indicating that STIM1 phosphorylation could be considered a potential therapeutic target against tumor progression.

2 . Materials and methods

2.1. Materials

EGF was purchased from Sigma; DMEM, RPMI 1640, FBS, and NuPAGE Bis-Tris gels were from Life Technologies; PD0325901 from Axon Medchem BV (Groningen, The Netherlands); fura-2-acetoxymethyl ester (fura-2-AM) was from Calbiochem (a Merck brand, Darmstadt, Germany); thapsigargin (Tg) and SKF96365 were from AbCam Biochemicals (Cambridge, UK); SuperSignal substrate for chemiluminescence was from Thermo Scientific; GFP-Trap resin was from Chromotek GmbH (Planegg-Martinsried, Germany); protein G-sepharose was from Santa Cruz Biotechnology; polyethylenimine was purchased from Polysciences, Inc. (Eppelheim, Germany).

2.2. DNA constructs

DNA constructs for transient expression of STIM1, EB1, STIM1-S575A/S608A/S621A, and STIM1-S575E/S608E/S621E tagged with either Flag-, GFP-, or mCherry-, have been described elsewhere [23,35]. DNA constructs were verified by DNA sequencing using BigDye Terminator v3.1 cycle sequencing protocol (Life Technologies) at the DNA Sequencing Unit of STAB, University of Extremadura (Spain). The construct for the transient expression of active H-Ras (H-RasG12V, construct DU20700) was from the Division Signal Transduction and Therapy (DSTT), University of Dundee, UK.

2.3. Antibodies

Phospho-specific antibodies raised against phospho-Ser575-STIM1, phospho-Ser608-STIM1, and phospho-Ser621-STIM1 were produced in collaboration with the Division of Signal Transduction Therapy (DSTT), University of Dundee, UK. The specificity of these antibodies has been reported elsewhere [23,35]. Antibodies against phosphorylated (phospho-Thr202/Tyr204) and total forms of ERK1/2 (raised in rabbit), and the rabbit anti-GFP antibody were from Cell Signaling Technology (Danvers, MA, USA). The rabbit polyclonal anti-STIM1 antibody was from ProSci Inc. (Poway, CA, USA). The rabbit anti-EB1 antibody (H-70) was from Santa Cruz Biotechnology. Anti-vimentin (Clone V9) was from Sigma-Aldrich (St. Louis, MO, USA), and anti-E-cadherin was from BD Biosciences (San Jose, CA, USA).

2.4. Cell culture

Ishikawa cells were obtained from the European Collection of Cell Cultures (ECACC). Cells were cultured in Dulbecco's modified Eagle's medium (DMEM) with 5% (v/v) fetal bovine serum (FBS), 2 mM L-glutamine, 100 U/ml penicillin, and 0.1 mg/ml streptomycin. Transfection of cells was performed with 1–2 μg plasmid DNA per 10-cm dish and polyethylenimine in serum-containing medium, 24–36 h prior to the beginning of the experiments. During the last 12 h, cells were cultured in FBS-free, phenol red-free RPMI 1640 medium supplemented with 2 mM L-glutamine, 100 U/ml penicillin, and 0.1 mg/ml streptomycin.

2.5. Cell migration assays

In vitro wound-healing assays were performed in 35-mm dishes at 80% cell confluence. The cell monolayer was scratched with a pipette tip (~500 μm width). Cells were photographed under phase contrast microscopy (time 0) and cultured as described above for the following 24 h. Thereafter, cells were photographed and quantitative image analysis of the wound healing was performed with ImageJ software.

2.6. Cell lysis and immunoblot

Cells were cultured for 12 h in FBS-free and phenol red-free RPMI 1640 medium before performing the experiments. After every treatment, cells were immediately placed on ice, washed with ice-cold PBS, and lysed. The lysis buffer was 50 mM Tris–HCl (pH 7.5), 1 mM EGTA, 1 mM EDTA, 1% (w/v) Igepal, 1 mM sodium orthovanadate, 50 mM sodium fluoride, 5 mM sodium pyrophosphate, 0.27 M sucrose, 0.1% (v/v) 2-mercaptoethanol, 1 mM benzamidine, and 0.1 mM phenylmethanesulfonyl fluoride. Clarification was performed after lysis with 1 ml of ice-cold lysis buffer per 10 cm-diameter dish, and centrifugation at 4 °C for 15 min at 20 000 *g*. Protein concentration was determined using the Bradford reagent (Thermo) and measuring the absorbance at 595 nm. Samples were reduced by the addition of 10 mM DTT followed by heating at 90 °C for 4 min before subjecting them to electrophoresis on 8–10% polyacrylamide Bis-Tris gels. Protein samples were electroblotted onto nitrocellulose membranes, and assessed with the following antibodies: anti-STIM1 (1 μg/ml), anti-phosphoSer575-STIM1 (1 μg/ml), anti-phosphoSer608-STIM1 (1 μg/ml), anti-phosphoSer621-STIM1 (1 μg/ml), anti-phospho-ERK1/2 (1 μg/ml), anti-total-ERK1/2 (1 μg/ml),

anti-GFP (1.23 μg/ml), anti-EB1 (0.2 μg/ml), anti-E-cadherin (50 ng/ml), and anti-vimentin (1 μg/ml). All incubations were performed overnight at 4 °C, in blocking buffer, with gentle shaking. Specific secondary antibodies labeled with HRP were used at 1:10 000–20 000 dilution, for 1 h at room temperature.

2.7. Pull-down and immunoprecipitation

GFP-tagged STIM1 or EB1 were purified as indicated elsewhere [22,23]. Equilibrated GFP-Trap agarose beads (5 μl) were added to clarified cell lysates (3–6 mg), followed by incubation for 1 h at 4 °C with gentle shaking. In immunoprecipitation assays the beads were washed twice with 1 ml lysis buffer containing 0.5 M NaCl and twice with 50 mM Tris–HCl, 0.1 mM EGTA, pH 7.5. In co-immunoprecipitation assays, GFP-Trap beads were washed twice with 1 ml lysis buffer containing 0.15 M NaCl and twice with 50 mM Tris–HCl, 0.1 mM EGTA, pH 7.5. Proteins were eluted from the beads by the addition of 7 μl NuPAGE-LDS sample buffer to the beads. Eluted proteins were reduced by the addition of 10 mM DTT followed by heating at 90 °C for 4 min. Luminol substrate was added and membranes were exposed to chemiluminescence films for 3 min. Developed films were scanned, and the signal was quantified by volumetric integration using ImageJ software. To immunoprecipitate untagged endogenous EB1, 1 mg of clarified Ishikawa cell lysate was incubated with 5 μg anti-EB1 antibody covalently conjugated to 5 μl protein G-sepharose overnight at 4 °C. The immunoprecipitates were washed twice with 5 ml lysis buffer containing 0.15 M NaCl and once with 5 ml buffer A. The beads were resuspended in sample buffer and subjected to electrophoresis on a 4–12% polyacrylamide gel, as indicated above.

2.8. Cytosolic free calcium concentration measurement

Cytosolic free calcium concentration ($[Ca^{2+}]_i$) was measured basically as described elsewhere [22,23,35]. Ishikawa cells growing on 18 mm-round glass coverslips were incubated with 2 μM fura-2-AM plus 0.025% Pluronic-F127 for 60 min in serum-free medium. The cells were then washed with Ca^{2+}-containing HBSS, and placed in the micro-incubation platform DH-40i (Warner Instruments, Hamden, CT, USA) of a Nikon TE2000 inverted microscope. Ratio fluorescence images were obtained with excitation filters of 340 and 380 nm, a 510 nm dichroic mirror, and a 520 nm emission filter (Semrock, Rochester, NY). Digital images were recorded with a Hamamatsu C9100-02 electron multiplier CCD camera, controlled by the Metafluor software. All measurements were made at 35 °C. Depletion of Ca^{2+} stores was triggered by incubating cells with 1 μM thapsigargin in Ca^{2+}-free HBSS with the following composition: 138 mM NaCl; 5.3 mM KCl; 0.34 mM Na_2HPO_4; 0.44 mM KH_2PO_4; 4.17 mM $NaHCO_3$; 4 mM $MgCl_2$; 0.1 mM EGTA (pH = 7.4). SOCE was measured by monitoring the increase of the $[Ca^{2+}]_i$ after the addition of 2 mM $CaCl_2$ to the Tg-containing medium [22,23,35].

2.9. Immunolocalization

Ishikawa cells were fixed in 4% paraformaldehyde for 10 min at room temperature. Then they were permeabilized with 0.2% Triton X-100 for 10 min and incubated in blocking solution (3% coldwater fish skin gelatin diluted in PBS-Tween 0.2%, pH 7.4) for 30 min at room temperature. Cells were incubated at room temperature for 1 h with the specific antibody, either anti-vimentin (1:50) or anti-E-cadherin (1:100) diluted in blocking solution, and then incubated at room temperature for 20 min with an anti-mouse IgG antibody labeled with Alexa Fluor-488 diluted 1:500 in blocking solution. Samples were counterstained with Hoechst 33342 (0.2 μg/ml) for 5 min, and were visualized by epifluorescence microscopy with a Superfluor 100× (NA 1.3) oil immersion objective in an inverted TE2000-U Nikon microscope.

2.10. Statistical analysis

Statistical analyses were done by the one-way analysis of variance (ANOVA). Differences between groups of data were considered statistically significant for $p < 0.05$. Values are represented as follows: $^{*}p < 0.05$, $^{**}p < 0.01$ and $^{***}p < 0.001$.

3 . Results

3.1. EGF activates Ca^{2+} influx in Ishikawa cells

In order to establish a protocol for studying STIM1 phosphorylation, and given that culturing cells in the presence of FBS stimulates diverse signaling pathways, we compared ERK1/2 activation in Ishikawa cells in two different culture media, DMEM and RPMI 1640, in the absence of FBS for 12 h (Fig. 1A). FBS deprivation is a common protocol with which to maintain low stimulation of cells in culture. We observed that FBS-free, phenol red-free RPMI 1640 avoided undesired activation of ERK1/2 activation during this time of incubation. For the following experiments, therefore, we cultured Ishikawa cells in FBS-supplemented DMEM until they reached the desired confluence, and then cells were incubated in FBS-free, phenol red-free RPMI 1640 for 12 h. Following this protocol we studied the activation of store-operated Ca^{2+} entry (SOCE) by Ca^{2+} store depletion triggered with thapsigargin (Tg) (Fig. 1B). Fura-2-loaded cells were treated with Tg, an inhibitor of the SERCA, in Ca^{2+}-free medium, and we observed the consequent release of Ca^{2+} from the endoplasmic reticulum, the Tg-sensitive intracellular Ca^{2+} store. The subsequent addition of Ca^{2+} to the assay medium revealed the increase of Ca^{2+} entry (SOCE) that was significantly inhibited by 10 μM SKF96365, a blocker of Ca^{2+} channels (Fig. 1B). At lower concentrations of SKF96365 (1 μM and 5 μM), the inhibition was partial.

As mentioned above, we had recently demonstrated that the phosphorylation of STIM1 by ERK1/2 regulates the activation of Ca^{2+} entry in HEK293 cells [22,23]. Because the ERK pathway is activated by EGF, we hypothesized that the EGF signaling pathway could be mediated by the phosphorylation of STIM1 under EGF-dependent ERK1/2 activation, and possibly by the activation of STIM1-dependent Ca^{2+} entry pathways. To test this hypothesis we measured the cytosolic free Ca^{2+} concentration ($[Ca^{2+}]_i$) in fura-2-loaded Ishikawa cells stimulated with EGF (10 ng/ml) (Fig. 1C–D) and we found that EGF elicited cytosolic Ca^{2+} spikes in Ca^{2+}-free medium, *i.e.* transient spikes of Ca^{2+} released from the intracellular stores. After 10 min of stimulation we added Ca^{2+} back to the assay medium, and observed a patent Ca^{2+} entry that was inhibited by 10 μM SKF96365, confirming the activation of Ca^{2+} entry by EGF in Ishikawa cells.

3.2. EGF triggers STIM1 phosphorylation and STIM1–EB1 dissociation

Following a similar experimental procedure, we monitored the activation of ERK1/2 by MEK1/2-dependent phosphorylation in Ishikawa cells stimulated with EGF. Using phospho-specific antibodies to detect pThr202/pTyr204-ERK1/2, we observed a significant activation of ERK1/2 after 10 min of stimulation with 10 ng/ml EGF in Ca^{2+}-free medium. This activation of ERK1/2 was fully prevented by PD0325901 (Fig. 2A), a recognized inhibitor of MEK1/2 [36]. Our results thus demonstrated that extracellular Ca^{2+} was not required to activate the MEK–ERK pathway in response to EGF stimulation. In parallel, we studied the phosphorylation profile of STIM1 at ERK1/2 target sites using phospho-specific antibodies against STIM1 residues Ser575, Ser608, and Ser621. We have recently reported the specificity of these antibodies, the absence of cross-reactivity, and the lack of sensitivity for the non-phosphorylated STIM1 [23,35]. Ishikawa cells were transfected for the transient expression of STIM1-GFP (wild type), and after 24 h of culture the cells were treated with 10 ng/ml EGF in Ca^{2+}-free medium for 10 min. Total lysates from these cells were used to pull-down

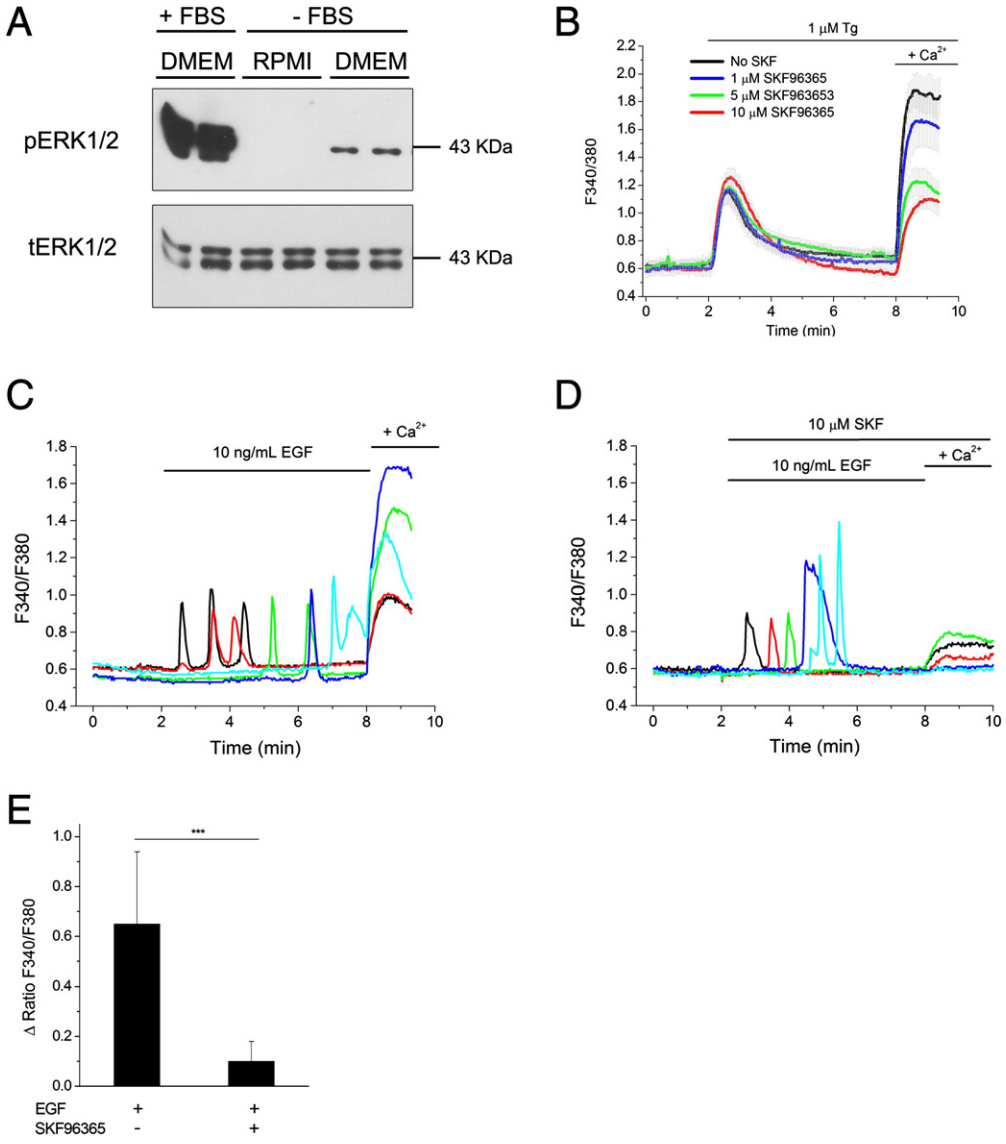

Fig. 1. EGF-triggered Ca^{2+} mobilization in Ishikawa cells. (A) Ishikawa cells were cultured in DMEM containing 5% FBS (first set of lanes), and then transferred to FBS-free, phenol red-free RPMI 1640 medium for 12 h (second set of lanes), or transferred to FBS-free DMEM (last set of lanes). Lysates from cells (20 μg) were subjected to electrophoresis and subsequent immunoblot using anti-phospho-Thr202/Tyr204-ERK1/2 (labeled as pERK1/2, upper panel) and anti-total-ERK1/2 antibodies to evaluate activation of ERK1/2. (B) SOCE was evaluated in fura-2-loaded Ishikawa cells after the addition of 1 μM thapsigargin (Tg) in Ca^{2+}-free HBSS followed by the addition of 2 mM $CaCl_2$ to the assay medium. The ratio F340/F380 was monitored by epifluorescence as indicated in Materials and Methods. SKF96365, at the indicated concentrations, was added together with Tg. Traces are mean ± s.d. of 4 independent experiments (>60 cells per experimental condition). Fura-2-loaded Ishikawa cells were treated with 10 ng/ml EGF in Ca^{2+}-free HBSS. After 6 min, 2 mM $CaCl_2$ was added to the assay medium, in the absence (C) or presence (D) of 10 μM SKF96365. Data are representative traces of 4 independent experiments (>30 cells per experimental condition). (E) The increase in the F340/F380 ratio after Ca^{2+} addition was evaluated from the experiment shown in panels C–D.

STIM1-GFP and to monitor the level of phospho-Ser575, phospho-Ser608 and phospho-Ser621 by immunoblot (Fig. 2B). The quantification of these immunoblots showed that EGF significantly stimulated the phosphorylation of STIM1 at Ser575, Ser608, and Ser621 after 10 min (Fig. 2C), demonstrating that STIM1 phosphorylation at ERK1/2 target sites was concomitant with the activation of the MEK–ERK pathway by EGF, and that this phosphorylation occurred in the absence of extracellular Ca^{2+}, *i.e.*, Ca^{2+} entry is not required to trigger either the activation of ERK1/2 or STIM1 phosphorylation at ERK1/2 target sites upon EGF stimulation. Moreover, PD0325901 prevented STIM1 phosphorylation, further demonstrating the role of ERK1/2 in STIM1 phosphorylation in Ishikawa cells stimulated with EGF.

Fig. 2. EGF triggers phosphorylation of STIM1 at ERK1/2 target sites. (A) Ishikawa cells were treated with 10 ng/ml EGF in Ca^{2+}-free HBSS for 10 min. Total lysates were used to evaluate phospho-ERK1/2 by immunoblot. Loading control was monitored with an anti-total-ERK1/2 antibody (lower blot). As a control of the experiment, cells were incubated with the ERK1/2 inhibitor PD0325901 (0.5 μM). Blots are representative of 3 independent experiments with 3 different lysates. (B) As in panel A, Ishikawa cells transfected for the transient expression of STIM1-GFP were treated with 10 ng/ml EGF in Ca^{2+}-free HBSS for 10 min. Total lysates were used to evaluate phospho-Ser575-STIM1, phospho-Ser608-STIM1, and phospho-Ser621-STIM1 by immunoblot. Total level of STIM1-GFP was evaluated with an anti-GFP antibody. In parallel, the determination of the level of ERK1/2 stimulation was performed by immunoblot, as in panel A. Total ERK1/2 levels were also monitored as loading control. Blots are representative of 4 independent experiments with 4 different lysates. (C) Quantification of the phosphorylated STIM1 observed in blots from panel B was performed by blot densitometry after subtracting the background for each blot lane, using ImageJ software. Data correspond to the calculated mean ± s.d. (D) Ishikawa cells were co-transfected for the transient expression of STIM1-GFP and H-Ras(G12V), and after 24 h cell lysates were assessed for phospho-Ser575-STIM1, phospho-Ser608-STIM1, and phospho-Ser621-STIM1 by immunoblot. Incubation of cells with PD0325901 (0.5 μM) was carried out in the 20 min before cell lysis. Total levels of STIM1-GFP were also evaluated with an anti-GFP antibody. The determination of phospho-ERK1/2 and total ERK1/2 levels was performed as in panel B. Blots are representative of 3 independent experiments with 3 different lysates.

These results are in accordance with the observation that overexpression of the GTPase H-Ras(G12V), a constitutively active mutant of H-Ras, leads to the increase of STIM1 phosphorylation at ERK1/2 target sites (Fig. 2D). H-Ras, also known as $p21^{ras}$, is an upstream activator of the Raf–MEK–ERK signal transduction pathway, and an essential mediator for EGF-dependent activation of this signaling pathway [37]. In addition, the phosphorylation of STIM1 triggered by H-Ras(G12V) was largely attenuated by PD0325901, confirming the role of ERK1/2 in this phosphorylation.

On the other hand, we have recently reported that phosphorylation of STIM1 at Ser575, Ser608, and Ser621 triggers its dissociation from

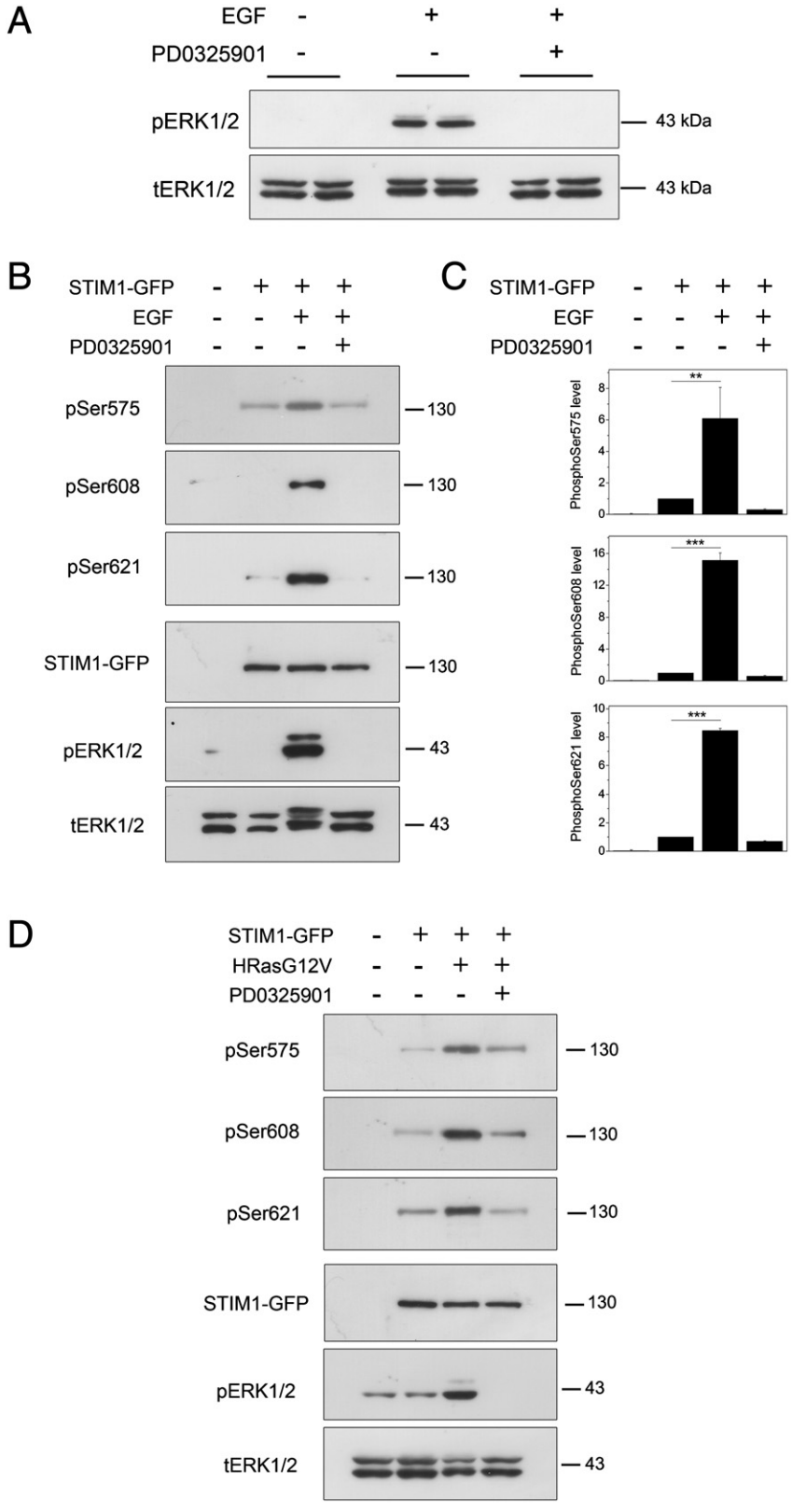

end-binding protein 1 (EB1) [23], a regulator of the growth of microtubule plus-ends [27,28]. However, our previous findings were observed in cells treated with Tg, a severe but non-physiological stimulus. Here, we investigated whether EGF triggered STIM1–EB1 dissociation by transfecting Ishikawa cells with EB1-GFP and Flag-STIM1, and stimulating cells with 10 ng/ml EGF. We then pulled-down EB1-GFP and studied the level of co-precipitated Flag-STIM1 by immunoblot (Fig. 3A). The results indicated that EGF stimulated the dissociation of STIM1 from EB1. This result was also supported by the observed dissociation between STIM1–EB1 when we immunoprecipitated endogenous EB1 and studied co-immunoprecipitated endogenous STIM1 (Fig. 3B). Therefore our results provide evidence that the MEK–ERK–STIM1 pathway becomes activated by EGF, and that this activation releases STIM1 from microtubule tips, a key event for the activation of SOCE [23].

The present result is also novel, in the sense that it constitutes the first reported evidence for the phosphorylation of STIM1 by ERK1/2, and for STIM1–EB1 dissociation upon physiological stimulation.

3.3. Phosphorylation of STIM1 is required to trigger cell migration

Given the chemotactic activity of EGF on epithelial cells, we investigated the role of Ca^{2+} entry and STIM1 phosphorylation on the cell migration of Ishikawa cells in response to stimulation in wound-healing assays (Fig. 4). The potentiation of cell migration by EGF was inhibited by 1 μM SKF96365, a concentration of the inhibitor that partially blocked Ca^{2+} entry but did not have any detrimental effect on cell viability. Interestingly, the ERK1/2 inhibitor PD0325901 also significantly blocked EGF-stimulated cell migration (Fig. 4A). These two results, together with the fact that EGF triggers the phosphorylation of STIM1, suggested a role for STIM1 phosphorylation in the control of cell migration. To study this hypothesis further, we transiently transfected Ishikawa cells for the expression of: (i) Flag-STIM1 (wild type); (ii) Flag-STIM1-S575A/S608A/S621A, *i.e.*, with Ser-to-Ala substitution mutations at ERK1/2 target sites, in order to mimic constitutive dephosphorylation at those sites; and (iii) Flag-STIM1-S575E/S608E/S621E, to mimic constitutive phosphorylation of STIM1. After 24 h, cells were assessed for cell migration in wound-healing assays, and we found that the overexpression of STIM1-S575A/S608A/S621A significantly inhibited cell migration stimulated by EGF (Fig. 4A). On the contrary STIM1-S575E/S608E/S621E normalized cell migration in wound-healing assays, confirming that the phosphorylation of STIM1 at ERK1/2 target sites regulates cell migration. In parallel, we analyzed the overexpressed STIM1 protein levels in this assay to ensure that this effect was not dependent on a level of protein expression that varied between different constructs. After monitoring the wound healing by phase contrast microscopy, cells were lysed, and total lysates were assessed for the evaluation of overexpressed Flag-STIM1 by immunoblot

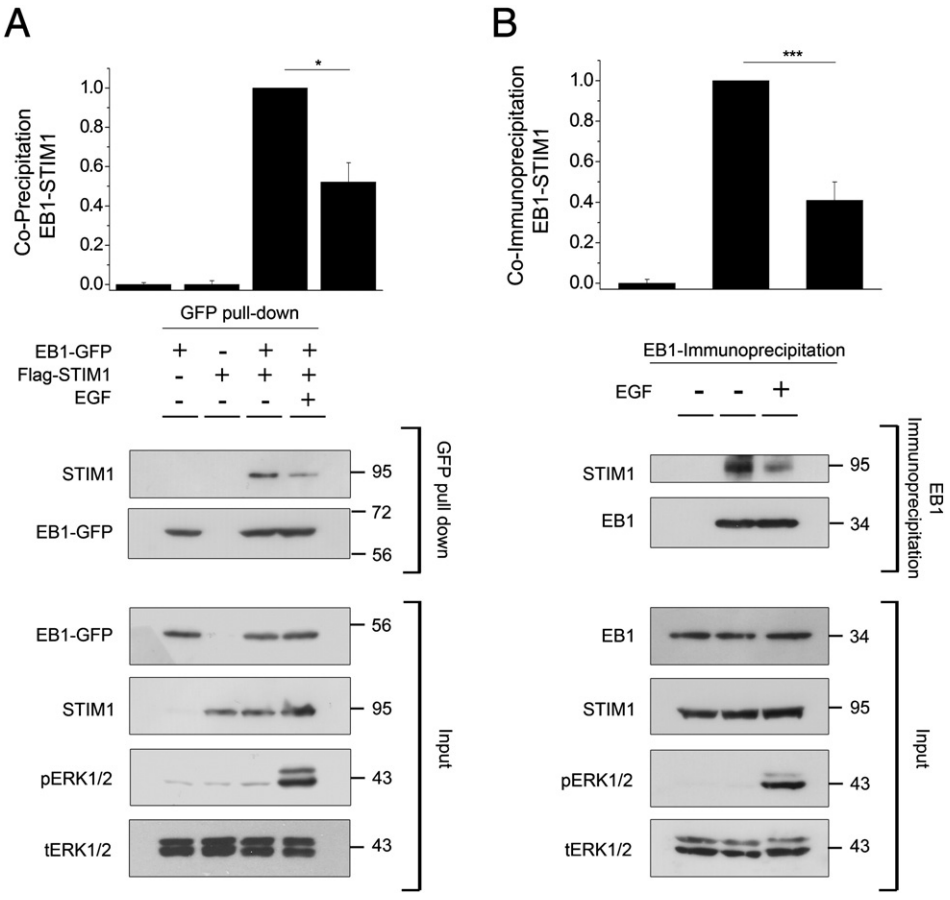

Fig. 3. EGF induces dissociation of STIM1 from EB1. (A) Ishikawa cells were transfected for transient expression of Flag-STIM1 and EB1-GFP. Twenty-four hours after transfection, cells were treated with 10 ng/ml EGF in Ca^{2+}-free HBSS for 10 min. GFP-tagged EB1 from these cells was pulled-down with GFP-Trap. The level of STIM1 bound to EB1 was evaluated by immunoblot using an anti-STIM1 antibody (upper panel), and the level of pulled-down EB1-GFP was evaluated with an anti-GFP antibody. Total amounts of EB1-GFP and Flag-STIM1 from lysates in each experimental condition are shown (input). Finally, to test ERK1/2 activation by EGF treatment, we monitored phospho-ERK1/2 and total ERK1/2. Quantification of STIM1–EB1 binding was performed by blot densitometry after subtracting the background for each blot lane, using ImageJ software. Blots are representative of 3 independent experiments with 3 different cultures. (B) Ishikawa cells were treated with 10 ng/ml EGF in Ca^{2+}-free HBSS for 10 min and endogenous EB1 from these cells was immunoprecipitated with an anti-EB1 antibody conjugated to protein G-sepharose. The level of immunoprecipitated EB1 was evaluated with the anti-EB1 antibody, and the level of co-immunoprecipitated STIM1 was evaluated with an anti-STIM1 antibody. As a negative control, lysates were incubated with protein G-sepharose in the absence of anti-EB1 antibody (first lane). Quantification of STIM1–EB1 co-immunoprecipitation was performed by blot densitometry, using ImageJ software. Blots are representative of 2 independent experiments with 2 different cultures.

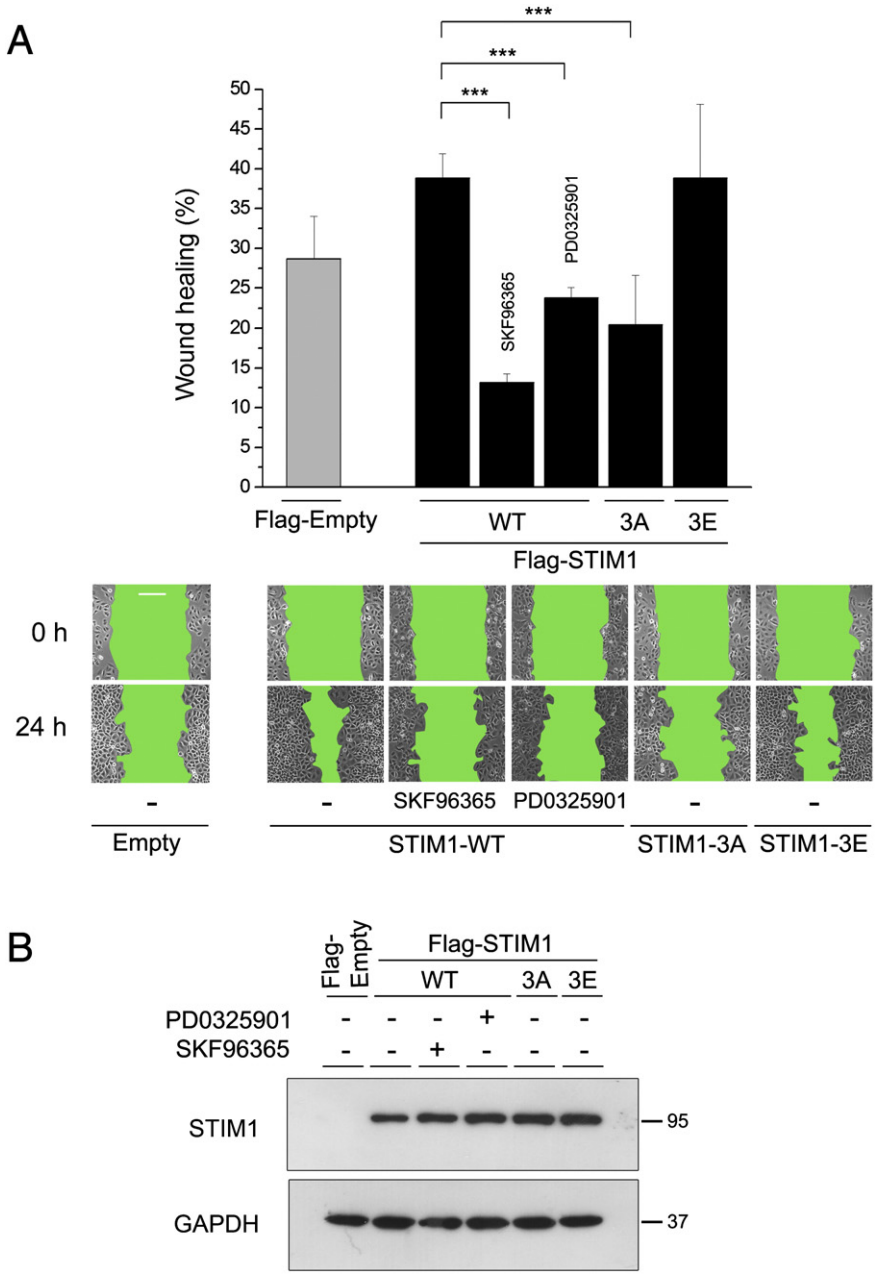

Fig. 4. Targeting STIM1 phosphorylation inhibits EGF-induced cell migration. (A) Ishikawa cells were transfected for the expression of Flag-STIM1, Flag-STIM1-S575A/S608A/S621A, or Flag-STIM1-S575E/S608E/S621E. Transfection with an empty vector was used as negative control. When cells reached 70% confluence, the cell monolayer was scratched and incubated with 10 ng/ml EGF for the following 24 h. When SKF96365 (1 μM) or PD0325901 (0.5 μM) was used, they were added to the culture medium together with EGF. Cells were photographed and quantitative image analysis was performed with ImageJ software. Data are presented as the mean ± s.d. of 4 independent experiments in triplicate. (B) After saving images from the experiment shown in panel A, total lysates of those cells were assessed for the expression of total STIM1 by immunoblot using an anti-STIM1 antibody in order to discard differences in STIM1 expression. Bar scale = 200 μm (shown for empty vector and time = 0).

(Fig. 4B). We observed an equal STIM1 expression for all the constructs used in this experiment under every experimental condition, confirming that dephosphorylation of STIM1 at ERK1/2 largely impairs cell migration.

3.4. STIM1 mediates the epithelial–mesenchymal transition triggered by EGF

It is known that EGF triggers an epithelial–mesenchymal transition (EMT) in Ishikawa cells [38], stimulating the decrease of epithelial markers and the concomitant increase of mesenchymal markers. Consequently, we hypothesized that the observed impaired migration of cells expressing Flag-STIM1-S575A/S608A/S621A might be due to a decreased EMT. To this end, we studied the profile of expression and localization of both E-cadherin and vimentin (two well recognized epithelial and mesenchymal markers) in Ishikawa cells treated with EGF. Fig. 5A shows that EGF triggers a significant switch in E-cadherin localization from subplasma membrane region to a more diffusely localization throughout the cytosol, as described for other epithelial cells which show that E-cadherin is sequestered into perinuclear vesicles during EMT [40]. Also, EGF triggered an increase of vimentin expression (see immunoblot in Fig. 5A) in well-defined cytoskeletal localization, in agreement with the behavior described for other epithelial cells upon EGF stimulation [39,40]. To evaluate the role of STIM1 phosphorylation

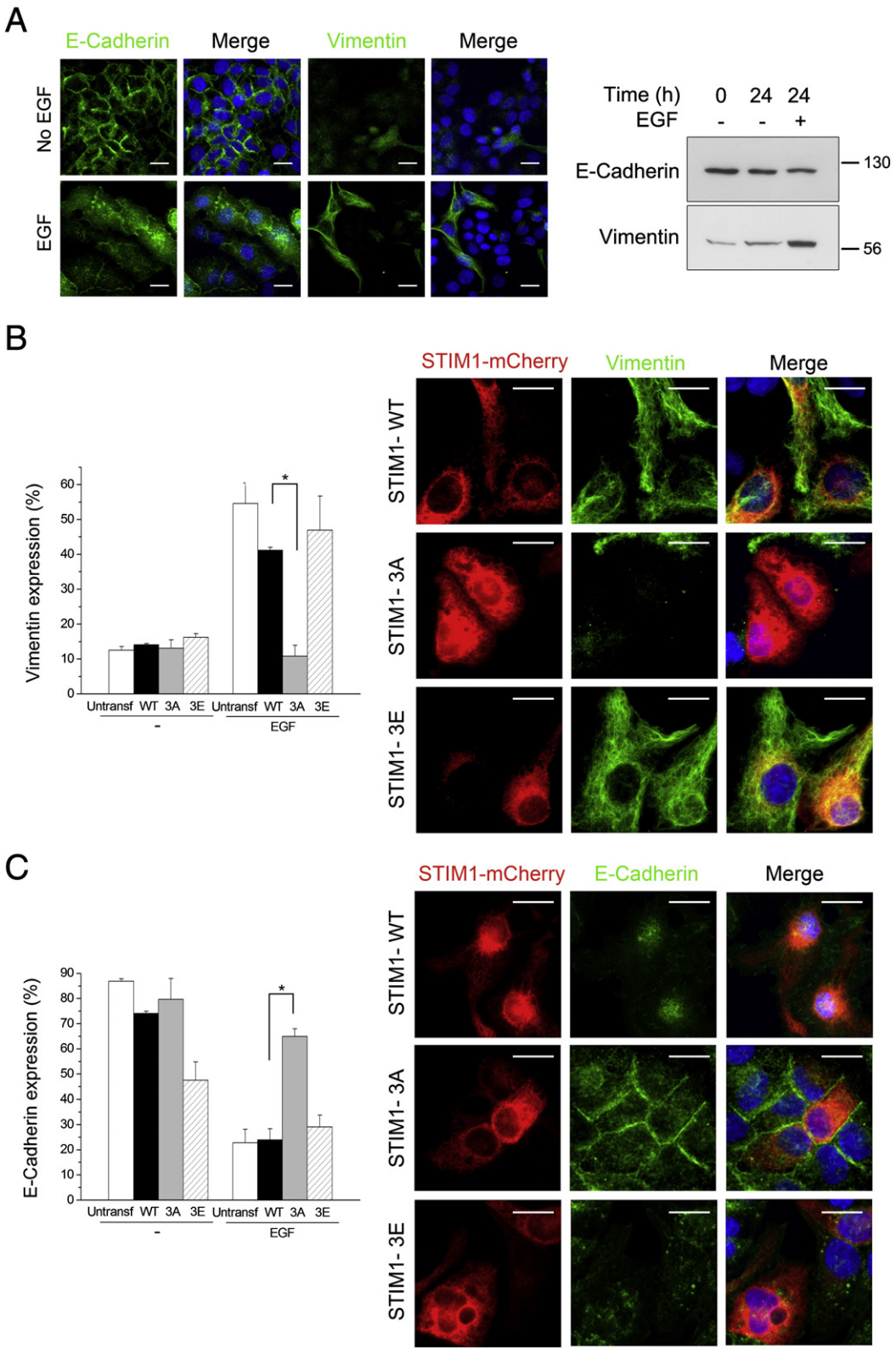

Fig. 5. Phosphorylation of STIM1 mediates EMT in Ishikawa cells. (A) The immunoblot and immunolocalization of vimentin or E-cadherin were performed to evaluate the level of expression and localization of these EMT markers in untreated cells *vs* EGF-treated cells (10 ng/ml for 24 h). Cells were counterstained with Hoechst 33342 for nuclei staining. Note that vimentin shows the typical intermediate filament profile, whereas E-cadherin shows a peripheral localization restricted to cell–cell junctions in unstimulated cells, and relocalized to the cytosol in EGF-treated cells. Bar scale = 20 μm. (B) The immunolocalization of vimentin was performed on Ishikawa cells transfected for the expression of STIM1-(wild type)-mCherry (black bar), STIM1-S575A/S608A/S621A-mCherry (gray bar), STIM1-S575E/S608E/S621E-mCherry (striped bar), and untransfected cells (white bar). Then, cells were stimulated with EGF as indicated in panel A. Within the STIM1-mCherry positive cells, we calculated vimentin-positive cells by counting randomly chosen fields (a minimum of 50 STIM1-mCherry-expressing cells per experiment), shown in bars. Representative images are shown of EGF-treated cells from this experiment. (C) Similarly, the immunolocalization of E-cadherin was performed on Ishikawa cells transfected for the expression of STIM1-(wt)-mCherry (black bar), STIM1-S575A/S608A/S621A-mCherry (gray bar), STIM1-S575E/S608E/S621E-mCherry (striped bar), and untransfected cells (white bar). Within the STIM1-mCherry positive cells, we evaluated the number of cells with peripheral localization of E-cadherin by counting randomly chosen fields (a minimum of 50 STIM1-mCherry-expressing cells per experiment), and representative images are shown of EGF-treated cells. Data are presented as the mean ± s.d. of 3 independent experiments performed in duplicate. Bar scale = 20 μm.

in the EGF-triggered EMT, we transfected Ishikawa cells for the transient expression of STIM1 (wild type)-mCherry, STIM1-S575A/S608A/S621A-mCherry, or STIM1-S575E/S608E/S621E-mCherry. After 24 h of stimulation with EGF, cells that expressed STIM1 (wild type)-mCherry showed a significant increase of vimentin expression and relocalized E-cadherin to the cytosol (Fig. 5B–C). However, cells overexpressing STIM1-S575A/S608A/S621A-mCherry did not show any significant increase in the expression of vimentin, whereas E-cadherin localization remained as in untreated cells. On the contrary, the overexpression of the phosphomimetic mutant STIM1-S575E/S608E/S621E-mCherry supported EMT equally as well as in cells transfected with STIM1-wild type-mCherry, *i.e.*, loss of filamentous E-cadherin and higher expression of vimentin in cells responding to treatment with EGF, confirming that phosphorylation of STIM1 at ERK1/2 sites mediates EMT in Ishikawa cells. The involvement in cell migration and EMT indicates that phosphorylation of STIM1 could merit consideration as a new pharmacological target for the treatment of cancer, a possibility that will need further experimental confirmation in animal models.

4 . Discussion

The Ras–Raf–MEK–ERK pathway is a downstream effector of tyrosine kinase receptors, including the epidermal growth factor receptor (EGFR), one of the most frequently mutated or overexpressed receptors in human cancers. Consequently, therapies that are based on targeting this signaling pathway have attracted the attention of current pharmacological investigation [29]. In this regard, activating mutations in the B-Raf isoform of the Raf kinase, or K-Ras isoform of the Ras protein are found in approximately 30% of all human cancers, with B-Raf(V600E) being the commonest B-Raf mutation in human carcinogenesis [41]. Therefore, many pre-clinical studies have focused on the use of specific inhibitors of the Raf–MEK–ERK pathway in order to evaluate their potential for the treatment of cancer. We have recently shown that STIM1 is a downstream target of ERK1/2 *in vitro* and *in vivo* [22,23], and that phosphorylation of STIM1 by ERK1/2 modulates Ca^{2+} entry by stimulating the dissociation of STIM1 from the microtubule plus-end-binding protein EB1 [23]. However, our previous findings were based on the inhibition of Ca^{2+} pumping into the ER, without the activation of any physiological pathway.

Ishikawa cells, derived from an endometrial adenocarcinoma, were used to show here for the first time that the activation of signaling pathways triggered by EGF leads to STIM1 phosphorylation at ERK1/2 target sites. In this regard, the present results prove that phosphorylation of STIM1 by ERK1/2 constitutes a way to activate STIM1 under physiological conditions (*i.e.*, EGF treatment), or upon oncogenic mutation of H-Ras, and not only by depleting Ca^{2+} stores with a SERCA inhibitor (thapsigargin). Also, our data show that STIM1–EB1 dissociation also occurs upon EGF stimulation, not only in response to the severe and non-physiological intraluminal Ca^{2+} depletion triggered by thapsigargin. In this regard, it has been shown that tubastatin-A, a specific histone deacetylase 6 (HDAC6) inhibitor, inhibits STIM1 relocalization and blocks SOCE activation in cancer cells [42], but did not affect the interaction between STIM1 and EB1, a result that fits well with the proposal that EB1-associated STIM1 does not activate Ca^{2+}-entry. Similarly, resveratrol inhibits the phosphorylation of STIM1, leading to the inhibition of the dissociation of STIM1 from EB1 and inhibition of SOCE in HEK293 cells [35]. Although we reported here that EGF triggers the dissociation of STIM1 from EB1, phosphorylation of STIM1 is reversible, and a Ca^{2+} entry-dependent STIM1 dephosphorylation was previously shown [23]. That means that there is cyclic phosphorylation/dephosphorylation, leading to a plausible binding back to EB1 when STIM1 becomes dephosphorylated. To test whether microtubules-mediated transport was responsible for the polarization of STIM1, Tsai et al. expressed an YFP-conjugated EB1-binding deficient mutant STIM1 (*i.e.*, mutated at Ile644/Thr645), and reporting that YFP-STIM1-Ile644Asn/Pro645Asn increased SOCE to a similar degree as wild type YFP-STIM1, indicating that the mutant maintained its full ability to control Ca^{2+} influx [7], as we reported previously in [23]. However, YFP-STIM1-Ile644Asn/Pro645Asn failed to polarize in migrating cells, suggesting the requirement of STIM1 to bind to EB1 at resting state, but not for the activation of SOCE. Thus, it is possible that STIM1 can travel bound to EB1 until reaching a restricted region of the cell with high Ras–Raf–MEK–ERK-activity, becoming phosphorylated, and then dissociating from EB1 to activate Ca^{2+} entry.

Another important conclusion that can be drawn from the results is that the activation of the MEK–ERK axis does not require the upstream activation of Ca^{2+} entry. On the contrary, we observed activation of ERK1/2 and phosphorylation of STIM1 at ERK1/2 target sites in the absence of extracellular Ca^{2+}. Therefore Ca^{2+} influx-independent phosphorylation of STIM1 triggered by EGF is an upstream event for STIM1-dependent cellular events, which constitutes strong support for the proposal that STIM1 phosphorylation modulates Ca^{2+}-entry. Indeed, STIM1 phosphorylation by ERK1/2 represents a positive feedback for the Raf–MEK–ERK pathway since it is known that the increase in intracellular Ca^{2+} levels mediates Ca^{2+}/calmodulin-dependent protein kinase II (CaMKII)-dependent activation of Raf-1 [43]. These data, together with the fact that Ishikawa cell migration is largely impaired by the Ca^{2+} channel blocker SKF96365 as well as by the ERK1/2 inhibitor PD0325901, led us to hypothesize that inhibition of STIM1 phosphorylation is sufficient to prevent cell migration. This hypothesis had yet to be explored, but was already supported by recent findings showing that the activation of receptor tyrosine kinase leads to local activation of STIM1 in the front of migrating endothelial cells [7].

As shown above, in this work we have described how targeting STIM1 phosphorylation constitutes a mechanism that impairs cell migration and epithelial–mesenchymal transition *in vitro*, strongly supporting a role for STIM1 phosphorylation in these cellular events. By transfecting Ishikawa cells for the expression of mutated STIM1 at ERK1/2 target sites, we have shown that constitutive dephosphorylation reduces the EGF-induced migration rate. Because dephosphorylated STIM1 remains inactive, our results are in agreement with the finding that knocking-down STIM1 expression, by using specific siRNA, prevents breast cancer cell migration and metastasis [11], and that Ca^{2+} influx activated by STIM1 is required for a proper turnover of focal adhesions [11]. Moreover, our results indicate that this specific phosphorylation of STIM1 modulates cell migration and the transformation to a mesenchymal-like phenotype, which explains the impairment of cell migration and EMT when STIM1 remains constitutively dephosphorylated. Because the knocking-down of STIM1 has been successfully used to prevent cell migration and metastasis, we consider that the phosphorylation of STIM1 on its modulatory domain is an alternative, easily druggable, target. At the cellular level, migration and invasion are strongly dependent on microtubule dynamics [44], and therefore microtubule polymerization has been considered a significant target in cancer therapy to reduce or prevent metastasis [45]. Many agents such as eribulin, ixabepilone, or cabazitaxel, are currently being used in phase III clinical trials. These agents either stabilize microtubules or interfere with microtubule polymerization [46–48]. However, the cytotoxicity of these drugs is significant as they block cell cycle at G2/M transition [47,49] and have a number of clinical side effects [50]. Thus, the ERK1/2-dependent phosphorylation of the cytosolic domain of STIM1 constitutes a potential targetable and restricted molecular motif that might be worthy of consideration in strategies intended to prevent cell migration and metastasis when designing new approaches to the treatment of human cancer.

In conclusion, we have here described solid evidence that EGF triggers phosphorylation of STIM1 at Ser575, Ser608, and Ser621, which are known targets of ERK1/2 activity. Also, STIM1 phosphorylation upon EGF stimulation triggers the dissociation of STIM1 from EB1, a key event in the activation of STIM1. Finally, by means of blocking phosphorylation of STIM1 or by mimicking this phosphorylation, we have

shown that phospho-STIM1 mediates EGF-triggered cell migration and EMT. This is the first report showing that STIM1 is a downstream effector of the Ras–Raf–MEK–ERK pathway and may contribute to the study of new roles for STIM1.

Acknowledgements

This work was supported by the Spanish Ministerio de Economía y Competitividad (Grant BFU2011-22798), Fundesalud (Grant PRIS11028), Gobierno de Extremadura (Grant GR10125 and PCJ1008), and European Social Fund. PTM was recipient of a predoctoral fellowship of the Junta de Extremadura (PD10081). AMLG was recipient of a predoctoral fellowship of the Spanish Ministerio de Economía y Competitividad (BES-2012-052061).

Appendix A. Supplementary data

Supplementary data to this article can be found online at http://dx.doi.org/10.1016/j.bbamcr.2014.10.027.

References

[1] R.S. Lewis, The molecular choreography of a store-operated calcium channel, Nature 446 (2007) 284–287.
[2] J. Liou, M. Fivaz, T. Inoue, T. Meyer, Live-cell imaging reveals sequential oligomerization and local plasma membrane targeting of stromal interaction molecule 1 after Ca2+ store depletion, Proc. Natl. Acad. Sci. U. S. A. 104 (2007) 9301–9306.
[3] M. Muik, I. Frischauf, I. Derler, M. Fahrner, J. Bergsmann, P. Eder, R. Schindl, C. Hesch, B. Polzinger, R. Fritsch, H. Kahr, J. Madl, H. Gruber, K. Groschner, C. Romanin, Dynamic coupling of the putative coiled-coil domain of ORAI1 with STIM1 mediates ORAI1 channel activation, J. Biol. Chem. 283 (2008) 8014–8022.
[4] A.V. Yeromin, S.L. Zhang, W. Jiang, Y. Yu, O. Safrina, M.D. Cahalan, Molecular identification of the CRAC channel by altered ion selectivity in a mutant of Orai, Nature 443 (2006) 226–229.
[5] J.P. Yuan, W. Zeng, G.N. Huang, P.F. Worley, S. Muallem, STIM1 heteromultimerizes TRPC channels to determine their function as store-operated channels, Nat. Cell Biol. 9 (2007) 636–645.
[6] S. Feske, Y. Gwack, M. Prakriya, S. Srikanth, S.H. Puppel, B. Tanasa, P.G. Hogan, R.S. Lewis, M. Daly, A. Rao, A mutation in Orai1 causes immune deficiency by abrogating CRAC channel function, Nature 441 (2006) 179–185.
[7] F.C. Tsai, A. Seki, H.W. Yang, A. Hayer, S. Carrasco, S. Malmersjo, T. Meyer, A polarized Ca2+, diacylglycerol and STIM1 signalling system regulates directed cell migration, Nat. Cell Biol. 16 (2014) 133–144.
[8] A. Somasundaram, A.K. Shum, H.J. McBride, J.A. Kessler, S. Feske, R.J. Miller, M. Prakriya, Store-operated CRAC channels regulate gene expression and proliferation in neural progenitor cells, J. Neurosci. 34 (2014) 9107–9123.
[9] M. Rodriguez-Moyano, I. Diaz, N. Dionisio, X. Zhang, J. Avila-Medina, E. Calderon-Sanchez, M. Trebak, J.A. Rosado, A. Ordonez, T. Smani, Urotensin-II promotes vascular smooth muscle cell proliferation through store-operated calcium entry and EGFR transactivation, Cardiovasc. Res. 100 (2013) 297–306.
[10] M. Li, C. Chen, Z. Zhou, S. Xu, Z. Yu, A TRPC1-mediated increase in store-operated Ca2+ entry is required for the proliferation of adult hippocampal neural progenitor cells, Cell Calcium 51 (2012) 486–496.
[11] S. Yang, J.J. Zhang, X.Y. Huang, Orai1 and STIM1 are critical for breast tumor cell migration and metastasis, Cancer Cell 15 (2009) 124–134.
[12] Y.F. Chen, W.T. Chiu, Y.T. Chen, P.Y. Lin, H.J. Huang, C.Y. Chou, H.C. Chang, M.J. Tang, M.R. Shen, Calcium store sensor stromal-interaction molecule 1-dependent signaling plays an important role in cervical cancer growth, migration, and angiogenesis, Proc. Natl. Acad. Sci. U. S. A. 108 (2011) 15225–15230.
[13] H. Liu, J.D. Hughes, S. Rollins, B. Chen, E. Perkins, Calcium entry via ORAI1 regulates glioblastoma cell proliferation and apoptosis, Exp. Mol. Pathol. 91 (2011) 753–760.
[14] R.K. Motiani, M.C. Hyzinski-Garcia, X. Zhang, M.M. Henkel, I.F. Abdullaev, Y.H. Kuo, K. Matrougui, A.A. Mongin, M. Trebak, STIM1 and Orai1 mediate CRAC channel activity and are essential for human glioblastoma invasion, Pflugers Arch. 465 (2013) 1249–1260.
[15] J. Yoshida, K. Iwabuchi, T. Matsui, T. Ishibashi, T. Masuoka, M. Nishio, Knockdown of stromal interaction molecule 1 (STIM1) suppresses store-operated calcium entry, cell proliferation and tumorigenicity in human epidermoid carcinoma A431 cells, Biochem. Pharmacol. 84 (2012) 1592–1603.
[16] N. Yang, Y. Tang, F. Wang, H. Zhang, D. Xu, Y. Shen, S. Sun, G. Yang, Blockade of store-operated Ca(2+) entry inhibits hepatocarcinoma cell migration and invasion by regulating focal adhesion turnover, Cancer Lett. 330 (2013) 163–169.
[17] M. Faouzi, F. Hague, M. Potier, A. Ahidouch, H. Sevestre, H. Ouadid-Ahidouch, Down-regulation of Orai3 arrests cell-cycle progression and induces apoptosis in breast cancer cells but not in normal breast epithelial cells, J. Cell. Physiol. 226 (2011) 542–551.
[18] F. Yu, L. Sun, S. Hubrack, S. Selvaraj, K. Machaca, Intramolecular shielding maintains the ER Ca(2)(+) sensor STIM1 in an inactive conformation, J. Cell Sci. 126 (2013) 2401–2410.
[19] M.K. Korzeniowski, I.M. Manjarres, P. Varnai, T. Balla, Activation of STIM1–Orai1 involves an intramolecular switching mechanism, Sci. Signal. 3 (2010) ra82.
[20] F. Yu, L. Sun, K. Machaca, Orai1 internalization and STIM1 clustering inhibition modulate SOCE inactivation during meiosis, Proc. Natl. Acad. Sci. U. S. A. 106 (2009) 17401–17406.
[21] J.T. Smyth, J.G. Petranka, R.R. Boyles, W.I. DeHaven, M. Fukushima, K.L. Johnson, J.G. Williams, J.W. Putney Jr., Phosphorylation of STIM1 underlies suppression of store-operated calcium entry during mitosis, Nat. Cell Biol. 11 (2009) 1465–1472.
[22] E. Pozo-Guisado, D.G. Campbell, M. Deak, A. Alvarez-Barrientos, N.A. Morrice, I.S. Alvarez, D.R. Alessi, F.J. Martin-Romero, Phosphorylation of STIM1 at ERK1/2 target sites modulates store-operated calcium entry, J. Cell Sci. 123 (2010) 3084–3093.
[23] E. Pozo-Guisado, V. Casas-Rua, P. Tomas-Martin, A.M. Lopez-Guerrero, A. Alvarez-Barrientos, F.J. Martin-Romero, Phosphorylation of STIM1 at ERK1/2 target sites regulates interaction with the microtubule plus-end binding protein EB1, J. Cell Sci. 126 (2013) 3170–3180.
[24] O. Thastrup, P.J. Cullen, B.K. Drobak, M.R. Hanley, A.P. Dawson, Thapsigargin, a tumor promoter, discharges intracellular Ca(2+) stores by specific inhibition of the endoplasmic reticulum Ca(2+)-ATPase, Proc. Natl. Acad. Sci. U. S. A. 87 (1990) 2466–2470.
[25] L. Vaca, SOCIC: the store-operated calcium influx complex, Cell Calcium 47 (2010) 199–209.
[26] I. Grigoriev, S.M. Gouveia, B. van der Vaart, J. Demmers, J.T. Smyth, S. Honnappa, D. Splinter, M.O. Steinmetz, J.W. Putney Jr., C.C. Hoogenraad, A. Akhmanova, STIM1 is a MT-plus-end-tracking protein involved in remodeling of the ER, Curr. Biol. 18 (2008) 177–182.
[27] J.S. Tirnauer, B.E. Bierer, EB1 proteins regulate microtubule dynamics, cell polarity, and chromosome stability, J. Cell Biol. 149 (2000) 761–766.
[28] L. Berrueta, S.K. Kraeft, J.S. Tirnauer, S.C. Schuyler, L.B. Chen, D.E. Hill, D. Pellman, B.E. Bierer, The adenomatous polyposis coli-binding protein EB1 is associated with cytoplasmic and spindle microtubules, Proc. Natl. Acad. Sci. U. S. A. 95 (1998) 10596–10601.
[29] P.J. Roberts, C.J. Der, Targeting the Raf–MEK–ERK mitogen-activated protein kinase cascade for the treatment of cancer, Oncogene 26 (2007) 3291–3310.
[30] S. Giambartolomei, F. Covone, M. Levrero, C. Balsano, Sustained activation of the Raf/MEK/Erk pathway in response to EGF in stable cell lines expressing the Hepatitis C Virus (HCV) core protein, Oncogene 20 (2001) 2606–2610.
[31] S.J. Wang, W. Saadi, F. Lin, C. Minh-Canh Nguyen, N. Li Jeon, Differential effects of EGF gradient profiles on MDA-MB-231 breast cancer cell chemotaxis, Exp. Cell Res. 300 (2004) 180–189.
[32] M. Grande, A. Franzen, J.O. Karlsson, L.E. Ericson, N.E. Heldin, M. Nilsson, Transforming growth factor-beta and epidermal growth factor synergistically stimulate epithelial to mesenchymal transition (EMT) through a MEK-dependent mechanism in primary cultured pig thyrocytes, J. Cell Sci. 115 (2002) 4227–4236.
[33] Z. Lu, S. Ghosh, Z. Wang, T. Hunter, Downregulation of caveolin-1 function by EGF leads to the loss of E-cadherin, increased transcriptional activity of beta-catenin, and enhanced tumor cell invasion, Cancer Cell 4 (2003) 499–515.
[34] M. Nishida, K. Kasahara, M. Kaneko, H. Iwasaki, K. Hayashi, Establishment of a new human endometrial adenocarcinoma cell line, Ishikawa cells, containing estrogen and progesterone receptors, Nihon Sanka Fujinka Gakkai Zasshi 37 (1985) 1103–1111.
[35] V. Casas-Rua, I.S. Alvarez, E. Pozo-Guisado, F.J. Martin-Romero, Inhibition of STIM1 phosphorylation underlies resveratrol-induced inhibition of store-operated calcium entry, Biochem. Pharmacol. 86 (2013) 1555–1563.
[36] J. Bain, L. Plater, M. Elliott, N. Shpiro, C.J. Hastie, H. McLauchlan, I. Klevernic, J.S. Arthur, D.R. Alessi, P. Cohen, The selectivity of protein kinase inhibitors: a further update, Biochem. J. 408 (2007) 297–315.
[37] A. Minden, A. Lin, M. McMahon, C. Lange-Carter, B. Derijard, R.J. Davis, G.L. Johnson, M. Karin, Differential activation of ERK and JNK mitogen-activated protein kinases by Raf-1 and MEKK, Science 266 (1994) 1719–1723.
[38] W.N. Yang, Z.H. Ai, J. Wang, Y.L. Xu, Y.C. Teng, Correlation between the overexpression of epidermal growth factor receptor and mesenchymal makers in endometrial carcinoma, J. Gynecol. Oncol. 25 (2014) 36–42.
[39] J.M. Lee, S. Dedhar, R. Kalluri, E.W. Thompson, The epithelial–mesenchymal transition: new insights in signaling, development, and disease, J. Cell Biol. 172 (2006) 973–981.
[40] L. Larue, A. Bellacosa, Epithelial–mesenchymal transition in development and cancer: role of phosphatidylinositol 3′ kinase/AKT pathways, Oncogene 24 (2005) 7443–7454.
[41] E.R. Cantwell-Dorris, J.J. O'Leary, O.M. Sheils, BRAFV600E: implications for carcinogenesis and molecular therapy, Mol. Cancer Ther. 10 (2011) 385–394.
[42] Y.T. Chen, Y.F. Chen, W.T. Chiu, K.Y. Liu, Y.L. Liu, J.Y. Chang, H.C. Chang, M.R. Shen, Microtubule-associated histone deacetylase 6 supports the calcium store sensor STIM1 in mediating malignant cell behaviors, Cancer Res. 73 (2013) 4500–4509.
[43] M. Salzano, M.R. Rusciano, E. Russo, M. Bifulco, L. Postiglione, M. Vitale, Calcium/calmodulin-dependent protein kinase II (CaMKII) phosphorylates Raf-1 at serine 338 and mediates Ras-stimulated Raf-1 activation, Cell Cycle 11 (2012) 2100–2106.
[44] P. Zhang, X. Ma, E. Song, W. Chen, H. Pang, D. Ni, Y. Gao, Y. Fan, Q. Ding, Y. Zhang, X. Zhang, Tubulin cofactor a functions as a novel positive regulator of ccRCC progression, invasion and metastasis, Int. J. Cancer 133 (2013) 2801–2811.
[45] D.A. Yardley, Activity of ixabepilone in patients with metastatic breast cancer with primary resistance to taxanes, Clin. Breast Cancer 8 (2008) 487–492.

[46] M.A. Jordan, K. Kamath, T. Manna, T. Okouneva, H.P. Miller, C. Davis, B.A. Littlefield, L. Wilson, The primary antimitotic mechanism of action of the synthetic halichondrin E7389 is suppression of microtubule growth, Mol. Cancer Ther. 4 (2005) 1086–1095.
[47] F.Y. Lee, R. Borzilleri, C.R. Fairchild, S.H. Kim, B.H. Long, C. Reventos-Suarez, G.D. Vite, W.C. Rose, R.A. Kramer, BMS-247550: a novel epothilone analog with a mode of action similar to paclitaxel but possessing superior antitumor efficacy, Clin. Cancer Res. 7 (2001) 1429–1437.
[48] X. Pivot, P. Koralewski, J.L. Hidalgo, A. Chan, A. Goncalves, G. Schwartsmann, S. Assadourian, J.P. Lotz, A multicenter phase II study of XRP6258 administered as a 1-h i.v. infusion every 3 weeks in taxane-resistant metastatic breast cancer patients, Ann. Oncol. 19 (2008) 1547–1552.
[49] M.J. Towle, K.A. Salvato, J. Budrow, B.F. Wels, G. Kuznetsov, K.K. Aalfs, S. Welsh, W. Zheng, B.M. Seletsky, M.H. Palme, G.J. Habgood, L.A. Singer, L.V. Dipietro, Y. Wang, J.J. Chen, D.A. Quincy, A. Davis, K. Yoshimatsu, Y. Kishi, M.J. Yu, B.A. Littlefield, In vitro and in vivo anticancer activities of synthetic macrocyclic ketone analogues of halichondrin B, Cancer Res. 61 (2001) 1013–1021.
[50] J.A. Yared, K.H. Tkaczuk, Update on taxane development: new analogs and new formulations, Drug Des. Dev. Ther. 6 (2012) 371–384.